



Published in final edited form as:

*J Comput Assist Tomogr.* 2015 ; 39(6): 907–913. doi:10.1097/RCT.0000000000000295.

## Quantitative and qualitative comparison of single source dual-energy CT and 120 kVp CT for the assessment of pancreatic ductal adenocarcinoma

**Priya Bhosale, MD,**

Department of Diagnostic Radiology, UT MD Anderson Cancer Center, Houston, TX

**Ott Le, MD,**

Department of Diagnostic Radiology, UT MD Anderson Cancer Center, Houston, TX

**Aprana Balachandran, MD,**

Department of Diagnostic Radiology, UT MD Anderson Cancer Center, Houston, TX

**Patricia Fox,**

Department of Biostatistics, UT MD Anderson Cancer Center, Houston, TX

**Eric Paulson, MD,** and

Department of Diagnostic Radiology, UT MD Anderson Cancer Center, Houston, TX

**Eric Tamm, MD**

Department of Diagnostic Radiology, UT MD Anderson Cancer Center, Houston, TX

### Abstract

**Purpose**—To compare contrast-to-noise ratio (CNR) and signal-to-noise ratio (SNR) between pancreatic phase dual-energy computed tomography (DECT) and 120 kVp CT for pancreatic ductal adenocarcinoma (PDA).

**Materials and Methods**—78 patients underwent multiphase pancreatic imaging protocols for PDA (40, DECT and 38, 120 kVp CT [control]). Using pancreatic phase, CNR and SNR for PDA were obtained for DECT at monochromatic energies (ME) 50 through 80 keV, iodine material density images (MDI), and 120 kVp images. Using a 5 point scale (1=excellent and 5=markedly limited) images were qualitatively assessed by two radiologist in consensus for PDA detection, extension, vascular involvement, and noise. Wilcoxon signed-rank and 2-sample tests were used to compare the qualitative measures, CNR, SNR for DECT and 120 kVp images. Bonferroni correction was applied.

**Results**—Iodine MDI had significantly higher CNR and SNR for PDA than any ME images ( $p < .0001$ ) and the 120 kVp images. Qualitatively 70 keV images were rated highest in the categories of tumor extension and vascular invasion and were similar to 120kVp images.

**Conclusion**—Our results indicate that DECT improves PDA lesion conspicuity compared to routine 120 kVp CT which may allow for better detection of PDA.

## Keywords

Pancreatic ductal adenocarcinoma; 120kVp; DECT; CNR and SNR

---

## Introduction

Pancreatic cancer is the 5th leading cause of cancer death worldwide and the 4th leading cause of cancer death in the United States. Surgery is considered the only means for cure, but for many patients surgery is contraindicated because disease at presentation is already either metastatic or too extensively involves critical vascular structures to make resection possible. Imaging plays a central role in this stratification of patients. The current practice in many institutions in the initial work up of patients with suspected pancreatic ductal adenocarcinomas (PDA) is to utilize a dedicated pancreatic protocol using conventional single energy MDCT scanner [1]. Multi-detector computed tomography (MDCT), during the phase of peak pancreatic enhancement (pancreatic parenchymal phase) has high diagnostic sensitivity for visualizing PDA >2 cm, but decreases in smaller lesions [2]. These small, sometimes isoattenuating, lesions may only demonstrate subtle secondary features such as pancreatic atrophy or pancreatic or biliary ductal dilation and therefore can be difficult to visualize and consequently manage [3, 4]. Such isoattenuating lesions are not infrequent on MDCT. One series reported that 11% of PDAs were isoattenuating to the pancreas [5] while another study reported that 27% of tumors <2 cm were isoattenuating to the pancreas [6]. Improving the visualization of PDA would therefore have a potentially significant impact on patient management.

Recent developments in CT have attempted to improve the conspicuity of PDA. A recent study showed that decreasing tube voltage (kVp) can increase the conspicuity of PDA by improving the conspicuity of contrast enhancement [7]. That image data from low (80–100kVp) and high (140kVp) energies can create a unique data set that can be used to generate low keV monochromatic images, which increase the conspicuity of enhancement of iodinated contrast, as well as material decomposition images (MDI). Iodine MDI also augments the conspicuity of enhancement of iodinated contrast and may be helpful in the visualization of pancreatic cancers. To our knowledge, only limited information is available in the literature regarding improving visualization of pancreatic tumors, particularly PDA, during the phase of peak pancreatic parenchymal enhancement with dual energy imaging through use of low keV monochromatic images or iodine MDI, and how those techniques compare with conventional MDCT imaging during the same phase. Lin et al. [8] showed improved conspicuity of hypervascular islet cell tumors for patients images with dual phase DECT (monochromatic and iodine MDI) compared to patients imaged with conventional multiphase MDCT, but did not evaluate PDA. Patel et. al. showed improved CNR on DECT for low keV images compared to high keV monochromatic images for PDA, but did not evaluate iodine MDI and did not compare it to conventional MDCT imaging.

The purpose of this study was to (1) compare the contrast to noise ratios (CNR) and signal to noise ratios (SNR) for PDA during the pancreatic parenchymal phase of imaging for DECT low energy (low keV) monochromatic images and/or iodine MDI to the conventional 120

kVp pancreatic parenchymal phase MDCT images scanned contemporaneously on similar patients. (2) Compare qualitative assessments by radiologists of these image sets with regard to such factors as tumor visualization, tumor extension, and vascular involvement.

## Materials and Methods

Following Institutional Review Board approval, institutional radiology databases were searched for patients who had and stage, untreated pathologically biopsy proven PDA and had undergone initial cross-sectional imaging staging at our institution either with DECT multiphase pancreas protocol or 120 kVp CT multiphase pancreas protocol examinations between November 2011 through February 2013. Patients who had prior therapy or did not have multiphase pancreatic protocol were excluded. Only patients who were adequately scanned at a display field of view (DFOV) of  $< 48$  were included. A total of 78 patients were identified. The routine images acquired at 120kVp were used as controls and were compared with the DECT images.

### Image Acquisition

During the period in question, pancreas protocol studies were acquired with either of two multiphase techniques, identical with regard to timing of phases, injection rate (with smart prep and a monitoring delay of 10 s and an aortic enhancement threshold of 100 Hounsfield units (HU) after administration of 125 mL of intravenous Optiray 350 at 4 mL/s), table speed (3.9cm), pitch (0.9), revolution time 1 sec, and slice reconstructions (2.5mm). They differed in that the pancreatic parenchymal phase was acquired with either a single source dual energy technique (64 detector row HD 750 Discovery CT scanner, Gemstone Spectral Imaging (GSI) General Electric, Milwaukee, WI) or a conventional/routine acquisition at 120kVp (64 detector row VCT, General Electric, Milwaukee, WI). These pancreatic parenchymal phase images in these two different cohorts of patients were then studied and compared. Patients underwent one technique or the other (DECT multiphase pancreas protocol or non DECT multiphase pancreas protocol) randomly depending on which technique was available at the location where they were scheduled to be scanned.

A “GSI preset” which had a fixed volume CT dose index ( $CTDI_{vol}$ ) output with fixed rotation speed was used as this was present on our scanners. Tube current modulation was not an option. The  $CTDI_{vol}$  for this phase on HD750 DECT was kept similar to that of our conventional 64 VCT. A sample of patients were assessed and sorted by the DFOV for each scanner to stratify them by size, and the  $CTDI_{vol}$  was identified for each. The population was divided into a smaller (DFOV  $< 42$ ) and larger (DFOV  $\geq 42$ ) and a GSI preset was chosen that corresponded to  $CTDI_{vol}$  values in the upper range of values for the two subpopulations. Higher  $CTDI_{vol}$  values were chosen for the following reasons. 1.  $> 80\%$  patients imaged at our institution are referred for suspicion of pancreatic cancer and ultimately have biopsy proven pancreatic adenocarcinoma. 2. These patients are considered potential surgical candidates and eventually undergo neoadjuvant or adjuvant radiation therapy. This justified the use of higher  $CTDI_{vol}$  value to optimize image quality for surgical staging and optimal management of the patients.

For both techniques, approximately 125–150cc of Omnipaque 350 was injected at 4–5cc/sec, to maintain injection duration of approximately 30 seconds. Bolus tracking was utilized, with a trigger value of 100 HU rise of the abdominal aorta (at approximately the level of the celiac), with a diagnostic delay of 20 seconds, such that in a normal patient, the scan would have started at the diaphragm approximately 40 seconds after the start of injection. Scan duration was approximately 5–7 seconds on both scanners. On both scanners, the portal venous phase was acquired 20 seconds later. Water was used as a negative contrast agent for both techniques. Only the pancreatic parenchymal phase images were reviewed in this study. These images were reconstructed at 2.5mm slice thickness as monochromatic images at 50 keV, 60 keV, 70 keV, and 80 keV values, as well as iodine MDI for the dual energy acquisition. For the 120kVp conventional acquisition, images were reconstructed also at 2.5mm. These sets of images were then transferred to a Philips iSite picture archiving communication system (Eindhoven, Netherlands) for purposes of review were placed in separate folders and blinded interpretation.

### Quantitative Evaluation

Two radiologists with dedicated experience in pancreatic cancer imaging at an oncologic center with 13 (PB) and 10(OL) years of experience separately evaluated the DECT and the 120 kVp images respectively. All images were quantitatively evaluated on the pancreatic parenchymal phase. The two radiologists evaluating the DECT images viewed 50, 60, 70, and 80 kVp together alongside the iodine MDI and placed the regions of interest (ROI) in the exact same locations. ROIs were placed by these radiologists which were 1cm in diameter, on the primary PDA and the non-tumoral pancreatic parenchyma. The HUs of the pancreas and the tumor as well as the standard deviation (SD) was recorded in an excel sheet. If the tumor was not seen then an ROI was placed where there was an abrupt cutoff of the pancreatic duct. Similarly, the ROIs of the subcutaneous fat were recorded in terms of HU and standard deviation. For tumor size measurements, the single largest diameter of the hypoattenuating mass on the axial plane was recorded. If no mass was seen, the size of the mass was documented as zero and excluded from comparisons of tumor size only. The location of the tumor was documented (pancreatic head body or tail).

### Qualitative Evaluation

Two radiologists ,one who helped with the quantitative measurement, and the other more experienced radiologist with dedicated experience in pancreatic imaging for 14 (AB) and 13 (PB) years respectively evaluated in consensus; the different DECT pancreatic parenchymal phase monochromatic energy image series and iodine MDI on an iSite picture archiving communication system (PACS). The images were reconstructed on the Advantage workstation at 50, 60, 70, or 80 keV and with iodine MDI and were sent to PACS. A hypodense area in the pancreas that caused pancreatic ductal dilation was considered a potential PDA and was evaluated in the following manner. The images were rated (1=excellent, 2=good, 3=fair, 4=poor and 5=markedly limited) in each of the following categories: visualization/detection of PDA, identification of tumor extension, vascular involvement, and image noise. All patients had pathologically proven PDA by biopsy.

## Statistical Analysis

Wilcoxon signed rank tests were used to compare the differences between paired DECT measurements. Wilcoxon-Mann Whitney tests were used to compare unpaired DECT and 120 kVp CT data. The Bonferroni correction was applied to p-values to adjust for multiple comparisons. Statistical analyses were performed using SAS 9.3© (SAS Institute Inc., Cary, NC, USA) software. P-values <0.0125 were considered significant after multiple comparison correction.

The contrast-to-noise ratio (CNR) was calculated as [(ROI) PDA-ROI of pancreas]/standard deviation (SD) of PDA and the signal-to-noise ratio (SNR) was calculated as (ROI) PDA/SD of pancreas. Fisher's exact test was used to see whether there was a difference between the size (diameter) and location of the tumors in patients who had the 120 kVp and DECT images.

## Results

### Patient Demographics

DECT scans were obtained for 40 patients, and multiphase pancreatic 120 kVp CT scans were obtained for 38 patients. For DECT, there were 15 women and 25 men, mean age 64 (range: 40–77). The mean tumor size on DECT was 3.36cm (SD=1.07) (range: 1.6–6.5 cm). The smallest tumor seen on DECT was 1.6cm. For the 120 kVp CT scans, there were 15 women and 23 men, and the mean age of the patients was 61 (range: 45–77). The mean size of the tumors on 120 kVp CT was 3.49 cm (SD=1.29) (range: 0–7 cm). Four PDAs were not seen on the 120 kVp CT images, and their sizes were documented as 0, however, the smallest visible tumor size seen was 1.7 cm. The size was not significantly different between the two groups of patients ( $p=0.64$ ), when the patients who did not have a visible tumor were excluded from tumor measurement analysis. Location of tumor was not statistically significantly different, fisher's exact  $p=0.55$ .

### Quantitative Analysis of CNR and SNR for DECT)

The iodine MDI provided significantly higher CNR for PDA than any of the other DECT image sets ( $p<0.0001$ ; Table 1; Fig 1&2). The 50, 60, and 70 keV images provided significantly higher CNR for PDA than the 80 keV images ( $p=0.0001$ ). No significant differences were observed between the 50, 60, and 70 keV energies for PDA CNR. The PDA SNR was higher for the iodine MDI than for the other DECT images (Table 1; Fig 3).

### CNR and SNR for DECT versus 120 kVp CT

The 50 keV, 60 keV, 70 keV, and iodine MDI provided significantly higher CNR for PDA than did 120 kVp CT ( $p<0.0001$ ,  $p<0.0001$ ,  $p<0.0005$ , and  $p<0.0001$ , respectively; Tables 1 and Fig 1). The 120 kVp CT had significantly lower pancreatic SNRs than the 50 keV, 70 keV, and iodine MDI (Table 1 and Fig 2).

The  $CTDI_{vol}$  and Dose length product (DLP) for the pancreatic parenchymal phase. For pancreatic phase 120kVp image the mean  $CTDI_{vol}$  was 22.9 mGy (maximum 38.0 and minimum 9.7mGy). The mean DLP was 740.8 mGy\*cm (max 1405.9 and minimum 286.9).

For pancreatic phase DECT the mean  $CTDI_{vol}$  was 28.3 mGy (maximum 38.1 and minimum 28.3mGy). The mean DLP was 861.5 mGy\*cm (maximum 1405.9 and minimum was 562.2 mGy\*cm).

### Qualitative analysis of DECT images

The iodine images were rated highest for visualizing or detecting primary PDA (Table 2). The 70 keV series was identified by readers qualitatively as the best to identify tumor extension (Table 3, Fig 4) and vascular invasion (Table 4). There was no difference in visualizing/detection of the primary tumor, tumor extension and vascular invasion between 120kVp and 70keV images (Fig 5). The 80 keV series had the least image noise (Table 5). Approximately 80% of the 50keV images were markedly limited whereas only 57.5% of the 60 keV images were rated as poor to -markedly limited (table5).

### Discussion

Our study suggests that CNRs for a hypoattenuating tumor such as PDA are better for low (e.g. 50–60) monochromatic energy images generated from dual energy data than CNRs for images generated by conventional MDCT polychromatic 120kVp imaging was confirmed in this study. Compared to standard 120 kVp CT, each of the monochromatic DECT energy series (50–70 keV) had significantly higher CNR for PDA except for 80 keV. As the K edge of iodine is 33.2 keV the attenuation of iodine on monochromatic energy images increases on lower keV monochromatic energy images. Thus, lower keV monochromatic energy images improve the conspicuity of enhancement of the tissues with iodinated contrast. For instance the pancreatic parenchyma appears intensely bright on lower keV images which increase the conspicuity of the hypoattenuating PDA [1]

Our study also confirmed that DECT iodine MDI had significantly higher CNR and SNR for PDA, than the 50, 60, 70, 80 keV DECT images studied. Our results therefore indicate that both DECT monochromatic energy imaging at low keV, and iodine MDI represent an improvement for CNR for PDA over conventional 120 kVp MDCT imaging, which we believe will likely improve PDA lesion conspicuity compared to routine 120 kVp CT and may facilitate better lesion detection and localization.

These findings are consistent with previously reported findings shown in other studies [9–11], that DECT may be superior to 120 kVp CT scans for the visualization of PDA. Other studies have suggested that DECT and perfusion DECT [10–12] help improve sensitivity for diagnosing pancreatic cancer [11, 12]. Patel et al demonstrated in 65 patients that the CNR of PDA was better on 45 keV images than on 70 keV images [13]. This is also concordant with findings by Brook et al.[14] (who used a different, single phase, split bolus, technique), at lower 60 keV, imaging improved contrast to noise ratios over high keV and over conventional MDCT. However, neither of these above mentioned groups evaluated the iodine MDI for CNR for PDA. Interestingly, our results are also similar to Lin [8], who studied a very different tumor type, pancreatic neuroendocrine tumors, which are typically hypervascular, compared to the typically hypovascular appearance of PDA. Similar to Lin et al [8], we found in our larger study that the CNR and SNR for PDA was the highest on the iodine MDI followed by the 50 keV image and that both iodine MDI and low keV imaging

improve CNR and SNR. We speculate that increased conspicuity of difference in contrast enhancement is helpful regardless of the tumor type.

Another novel feature of our study was having radiologists compare qualitatively images from various monochromatic energies (50 keV to 80 keV), and iodine MDI in regard to tumor conspicuity for detection of pancreatic cancers, degree of tumor extension, and visualization of the extent of vascular involvement. Prior studies have shown that monochromatic images at 51 keV improve image quality for intra and extra hepatic portal venography, improve CNR for vascular structures[15], and can aid assessment of large and small arteries over conventional MDCT owing to improved contrast[15–17] and image quality. In contrast, in our study, even though the 50 keV images were also noted to improve tumor conspicuity, they were rated subjectively as noisy, and readers noted that the more prominent enhancement of pancreatic parenchyma and adjacent vasculature at this lower keV overwhelmed subtle signs of peripancreatic PDA extension and vascular involvement (Tables 3 and 4). In our study, we found that subjective ratings indicated that the 70 keV images were probably the best to assess for vascular invasion and tumor extension. We speculate that this may have been because 70 keV images may have provided a perceived best balance of image noise, and soft tissue contrast with regard to assessing vascular involvement.

There are limitations to this study. First, it was a retrospective study comparing two different populations of patients with PDA undergoing baseline imaging prior to therapy, at presentation to our institution, one of which underwent conventional multiphase pancreas protocol imaging (polychromatic, 120 kVp) while the other underwent similar imaging with a dual energy technique. These patients were imaged during the same study time period, and were scheduled to one scanner or the other depending on which scanner happened to be available at the time of scheduling, not for any other reason, such as therapy, or disease status. However there was no statistically significant difference in the size and location of the PDA in both groups. Ethically it would not have been acceptable for the patients to have undergone two separate examinations, one at 120 kVp and the other DECT at the same setting for evaluation of PDA because of radiation dose issues as well as contrast administration issues. Another limitation is that we used a tiered approach of dose levels based on patient size, but had only two subgroups. More comparable dose levels could have been obtained with more subgroups. The newer GE GSI assist algorithms will help balance between image quality and radiation dose and this platform can be analyzed in the future.

Our study findings may have useful implications for imaging in other organs. We speculate that use of dual energy imaging may improve the conspicuity of typically hypodense metastatic disease to the liver from primary tumor such as colon cancer and improve visualization of washout of such tumors as hepatocellular carcinoma on portal venous phase or delayed phases of imaging. We found that 70 keV imaging was better for primary PDA staging, whereas low energy monochromatic energy images and iodine MDI were better for PDA detection. This information may be helpful for better evaluation and staging of PDA. Future directions of research may include studying additional types of material decomposition images, and studying how the various types of images created by dual energy

imaging can be used in daily practice in staging and detection and characterization of the different types and grades of PDA.

In conclusion, we found that monochromatic energy images specifically lower keV images and iodine MDI offer benefits over 120 kVp CT images for the detection and assessment of PDA based on the higher CNRs and SNRs. Additionally, the 70 keV images were rated by our readers qualitatively as the best (of the DECT images) and found to be statistically equivalent to the 120 kVp single energy CT images to evaluate tumor extension and vascular invasion.

## Acknowledgments

\*Supported by the NIH/NCI under award number P30CA016672- Cancer Center Support Grant.

## References

1. Kondo H, et al. MDCT of the pancreas: optimizing scanning delay with a bolus-tracking technique for pancreatic, peripancreatic vascular, and hepatic contrast enhancement. *AJR Am J Roentgenol.* 2007; 188(3):751–6. [PubMed: 17312064]
2. Pauls S, et al. Value of spiral CT and MRI (1.5 T) in preoperative diagnosis of tumors of the head of the pancreas. *Rontgenpraxis.* 2003; 55(1):3–15. [PubMed: 12650033]
3. Blouhos K, et al. Surgically proved visually isoattenuating pancreatic adenocarcinoma undetected in both dynamic CT and MRI. Was blind pancreaticoduodenectomy justified? *Int J Surg Case Rep.* 2013; 4(5):466–9. [PubMed: 23562894]
4. Kim JH, et al. Visually isoattenuating pancreatic adenocarcinoma at dynamic-enhanced CT: frequency, clinical and pathologic characteristics, and diagnosis at imaging examinations. *Radiology.* 2010; 257(1):87–96. [PubMed: 20697118]
5. Prokesch RW, et al. Isoattenuating pancreatic adenocarcinoma at multi-detector row CT: secondary signs. *Radiology.* 2002; 224(3):764–8. [PubMed: 12202711]
6. Yoon SH, et al. Small ( $\leq 20$  mm) pancreatic adenocarcinomas: analysis of enhancement patterns and secondary signs with multiphasic multidetector CT. *Radiology.* 2011; 259(2):442–52. [PubMed: 21406627]
7. Holm J, et al. Low tube voltage CT for improved detection of pancreatic cancer: detection threshold for small, simulated lesions. *BMC Med Imaging.* 2012; 12:20. [PubMed: 22828284]
8. Lin XZ, et al. Dual energy spectral CT imaging of insulinoma-Value in preoperative diagnosis compared with conventional multi-detector CT. *Eur J Radiol.* 2012; 81(10):2487–94. [PubMed: 22153746]
9. Macari M, et al. Dual-source dual-energy MDCT of pancreatic adenocarcinoma: initial observations with data generated at 80 kVp and at simulated weighted-average 120 kVp. *AJR Am J Roentgenol.* 2010; 194(1):W27–32. [PubMed: 20028887]
10. Xue HD, et al. Application of second generation dual-source computed tomography dual-energy scan mode in detecting pancreatic adenocarcinoma. *Zhongguo Yi Xue Ke Xue Yuan Xue Bao.* 2010; 32(6):640–4. [PubMed: 21219792]
11. He YL, et al. Clinical Value of Dual-energy CT in Detection of Pancreatic Adenocarcinoma: Investigation of the Best Pancreatic Tumor Contrast to Noise Ratio. *Chin Med Sci J.* 2013; 27(4): 207–12. [PubMed: 23294585]
12. Klauss M, et al. Dual-energy perfusion-CT of pancreatic adenocarcinoma. *Eur J Radiol.* 2013; 82(2):208–14. [PubMed: 23062281]
13. Patel BN, et al. Single-source dual-energy spectral multidetector CT of pancreatic adenocarcinoma: optimization of energy level viewing significantly increases lesion contrast. *Clin Radiol.* 2013; 68(2):148–54. [PubMed: 22889459]



14. Brook OR, et al. Split-bolus spectral multidetector CT of the pancreas: assessment of radiation dose and tumor conspicuity. *Radiology*. 2013; 269(1):139–48. [PubMed: 23674791]
15. Zhao LQ, et al. Improving image quality in portal venography with spectral CT imaging. *Eur J Radiol*. 2012; 81(8):1677–81. [PubMed: 21444170]
16. Vlahos I, et al. Dual-energy CT: vascular applications. *AJR Am J Roentgenol*. 2012; 199(5 Suppl):S87–97. [PubMed: 23097172]
17. Nakayama Y, et al. Abdominal CT with low tube voltage: preliminary observations about radiation dose, contrast enhancement, image quality, and noise. *Radiology*. 2005; 237(3):945–51. [PubMed: 16237140]

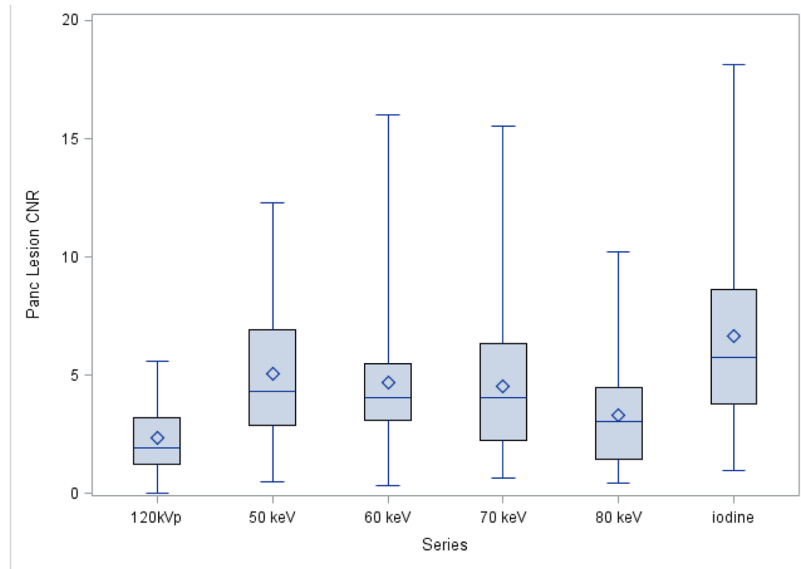


**Figure 1. Boxplot of Quantitative PDA-CNR by Series**

The symbol represents the mean and the line inside the box represents the median. The whiskers represent the minimum and maximum values. The box represents the middle 50% of the data

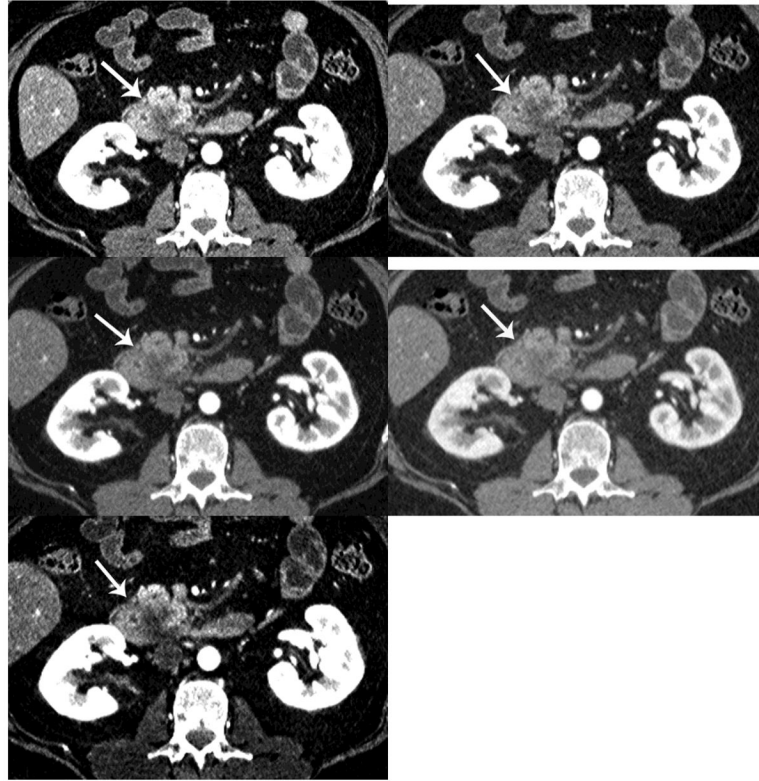


**Figure 2.** Detection of PDA. There is increased conspicuity of the PDA (arrow) with decreasing monochromatic energy levels (a=50keV, b=60keV, c=70keV, d=80keV and e=iodine MDI). The iodine material density image provides the best CNR.

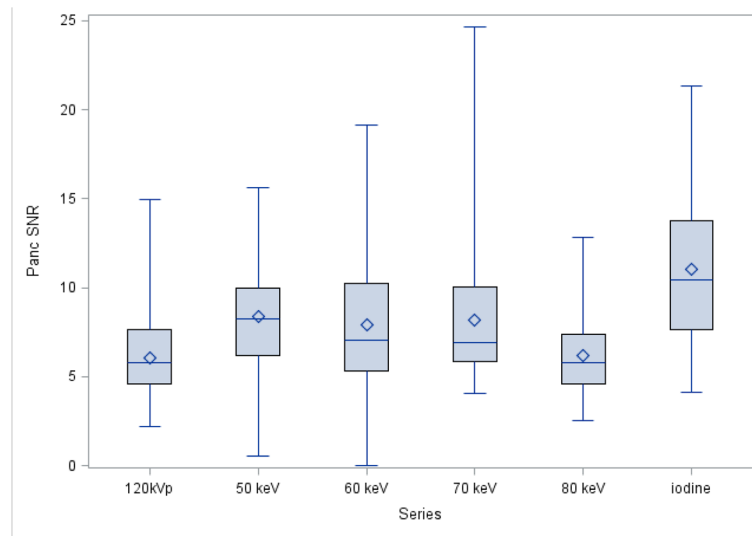


**Figure 3. Boxplot of Quantitative Pancreatic parenchyma SNR by Series**

The symbol represents the mean and the line inside the box represents the median. The whiskers represent the minimum and maximum values. The box represents the middle 50% of the data

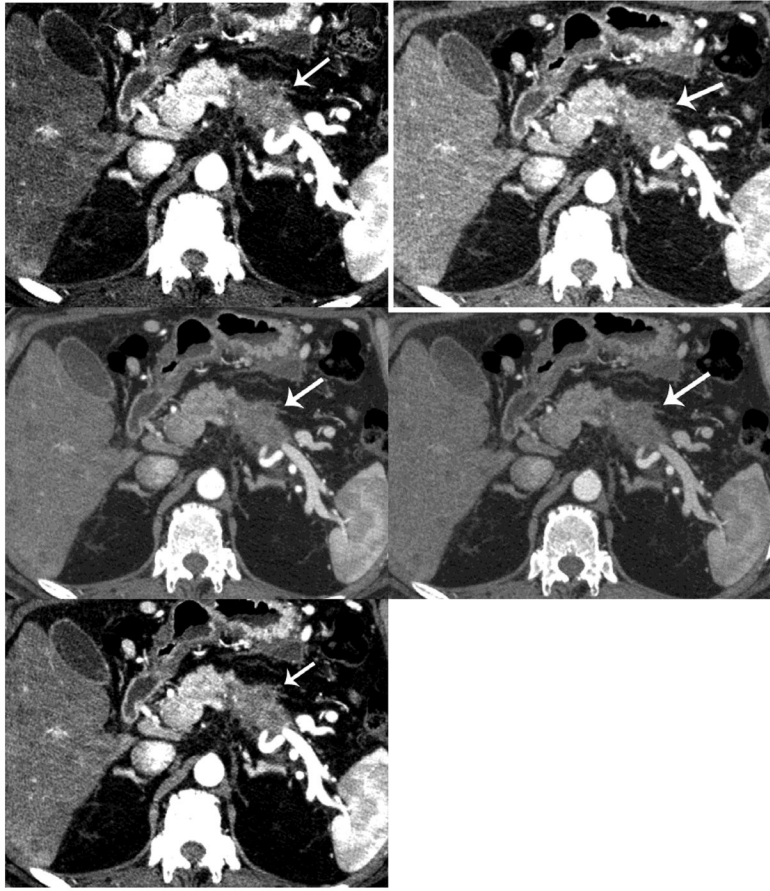


**Figure 4.** Vascular invasion/tumor spread. The 70 keV allows better visualization of the vascular anatomy in relation to the PDA (arrow) due to less noise. (a=50keV, b=60keV, c=70keV, d=80keV and e=iodine MDI)

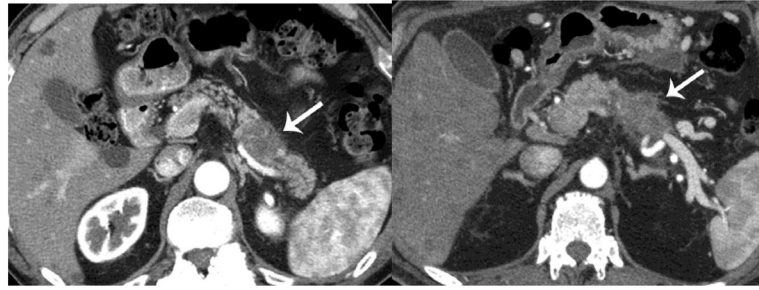


**Figure 5.** Qualitative comparisons between 120 kVp and 70 keV. When comparing the 70 keV to the 120 kVp series, there was no significant difference for visualization of the primary tumor (arrow), tumor extension, or vascular invasion, except for image noise

**Table 1**

Comparison of PDA CNR and SNR Values by Imaging Series

Variable	Imaging Series	N	Median	Minimum	Maximum
Lesion CNR <sup>a,b,c</sup>	50 keV	40	4.32	0.54	12.27
	60 keV	40	4.04	0.70	16.01
	70 keV	40	4.06	0.66	15.52
	80 keV	40	3.05	0.46	10.21
	Iodine	40	5.73	0.98	18.15
	120 kVp	38	1.93	0.01	5.57
	50 keV	40	8.24	3.11	15.63
	60 keV	40	7.04	1.00	19.16
SNR <sup>a,b,d</sup>	70 keV	40	6.93	4.05	24.68
	80 keV	40	5.81	2.51	12.83
	Iodine	40	10.46	4.14	21.36
	120 kVp	38	5.82	2.18	14.95

<sup>a</sup> 50, 60, and 70 keV had significantly higher lesion CNR and SNR than 80 keV (p<.0001)

<sup>b</sup> 50, 60, 70, and 80 keV had significantly lower lesion CNR and SNR than Iodine (p<.0001)

<sup>c</sup> 120 kVp had significantly lower CNR than 50, 60, 70 keV, and Iodine (p<.0001)

<sup>d</sup> 120 kVp had significantly lower SNR than 50,70 keV, and Iodine (p<.0001)

P-values incorporate the Bonferroni adjustment for multiple comparisons and the P-values <0.0125 are considered significant after multiple comparison correction

**Table 2**

Comparison of PDA Visualization Ratings in two different patient sets.

Variable	Rating	Imaging Series <sup>a,b,c,d,e</sup>					
		120 kVp	50 keV	60 keV	70 keV	80 keV	Iodine
Primary Tumor Visualization	Not rated			1(.%)	3(.%)	4(.%)	2(.%)
	Excellent	2(5%)		1(2.6%)	1(2.7%)		21(55.3%)
	Good	15(37.5%)		5(12.8%)	18(48.6%)	11(30.6%)	5(13.2%)
	Fair	14(35%)	10(25%)	17(43.6%)	10(27%)	11(30.6%)	6(15.8%)
	Poor	8(20%)	20(50%)	9(23.1%)	5(13.5%)	9(25%)	3(7.9%)
	Markedly limited	1(2.5%)	10(25%)	7(17.9%)	3(8.1%)	5(13.9%)	3(7.9%)

<sup>a</sup> 50 keV had significantly worse rating than 60, 70, 80, and Iodine (p<.0001)

<sup>b</sup> 60 keV had significantly worse rating than 70 keV and Iodine (p<.0001)

<sup>c</sup> 70 keV had significantly better rating than 80 keV (p=0.001) and iodine had higher ratings than 70keV (p<.0001)

<sup>d</sup> 80 keV had significantly worse rating than Iodine (p<.0001)

<sup>e</sup> 120 kVp was not significantly different than 70 keV (p=0.71)

P-values incorporate the Bonferromi adjustment for multiple comparisons.



**Table 3**

Comparison of Tumor Extension Visualization Ratings.

Variable	Rating	Imaging Series <sup>a,b,c</sup>					
		120 kVp	50 keV	60 keV	70 keV	80 keV	Iodine
Tumor Extension Visualization	Not rated			1(.%)	4(.%)	4(.%)	2(.%)
	Excellent	2(5%)			2(5.6%)		3(7.9%)
	Good	19(47.5%)		5(12.8%)	18(50%)	11(30.6%)	3(7.9%)
	Fair	11(27.5%)	10(25%)	18(46.2%)	9(25%)	10(27.8%)	14(36.8%)
	Poor	7(17.5%)	19(47.5%)	9(23.1%)	5(13.9%)	10(27.8%)	15(39.5%)
	Markedly limited	1(2.5%)	11(27.5%)	7(17.9%)	2(5.6%)	5(13.9%)	3(7.9%)

<sup>a</sup> 50 keV had significantly worse ratings than 60, 70, 80, and Iodine (p<.0001)

<sup>b</sup> 60 keV had significantly worse ratings than 70 keV (p<.0001)

<sup>c</sup> 70 keV had significantly better ratings than 80 keV and Iodine (p=0.0009 and 0.0012, respectively)

P-values incorporate the Bonferroni adjustment for multiple comparisons.

**Table 4**

Comparison of Vascular Invasion Visualization Ratings.

Variable	Rating	Imaging Series <sup>a,b,c,d</sup>					
		120 kVp	50 keV	60 keV	70 keV	80 keV	Iodine
Vascular Invasion Visualization	Not rated			1(.%)	2(.%)	4(.%)	3(.%)
	Excellent	2(5%)			1(2.6%)		3(8.1%)
	Good	23(57.5%)		5(12.8%)	21(55.3%)	15(41.7%)	2(5.4%)
	Fair	9(22.5%)	11(27.5%)	19(48.7%)	9(23.7%)	6(16.7%)	9(24.3%)
	Poor	5(12.5%)	19(47.5%)	8(20.5%)	4(10.5%)	10(27.8%)	19(51.4%)
	Markedly limited	1(2.5%)	10(25%)	7(17.9%)	3(7.9%)	5(13.9%)	4(10.8%)

<sup>a</sup> 50 keV had significantly worse ratings than 60, 70, and 80 keV (p<.0001)

<sup>b</sup> 60 keV had significantly worse ratings than 70 (p<.0001) and 80 keV (p=0.0011)

<sup>c</sup> 70 keV had significantly better ratings than 80 keV (p=0.002) and Iodine(p<.0001)

<sup>d</sup> 80 keV had significantly better ratings than Iodine (p=0.0029)

P-values incorporate the Bonferroni adjustment for multiple comparisons.

**Table 5**

Comparison of Image Noise Visualization Ratings.

Variable	Rating	Imaging Series <sup>a,b,c,d</sup>					
		120 kVp	50 keV	60 keV	70 keV	80 keV	Iodine
Image Noise Visualization	Not rated						
	Excellent	1(2.5%)			1(2.5%)	24(60%)	1(2.5%)
	Good	38(95%)		1(2.5%)	15(37.5%)	15(37.5%)	31(77.5%)
	Fair	1(2.5%)	6(15%)	16(40%)	19(47.5%)	1(2.5%)	6(15%)
	Poor		23(57.5%)	17(42.5%)	4(10%)		2(5%)
	Markedly limited		11(27.5%)	6(15%)	1(2.5%)		

<sup>a</sup> 50 keV had significantly worse ratings than 60, 70, 80, and Iodine (p<0.0001)

<sup>b</sup> 60 keV had significantly worse ratings than 70, 80 and iodine (p<0.0001)

<sup>c</sup> 70 keV had significantly worse ratings than 80 keV (p<.0001) and Iodine (p=0.0051)

<sup>d</sup> 80 keV had significantly better ratings than Iodine (p<0.0001)

P-values incorporate the Bonferroni adjustment for multiple comparisons.